Soft Matter

Accepted Manuscript

ROYAL SOCIETY OF CHEMISTRY

www.rsc.org/softmatter

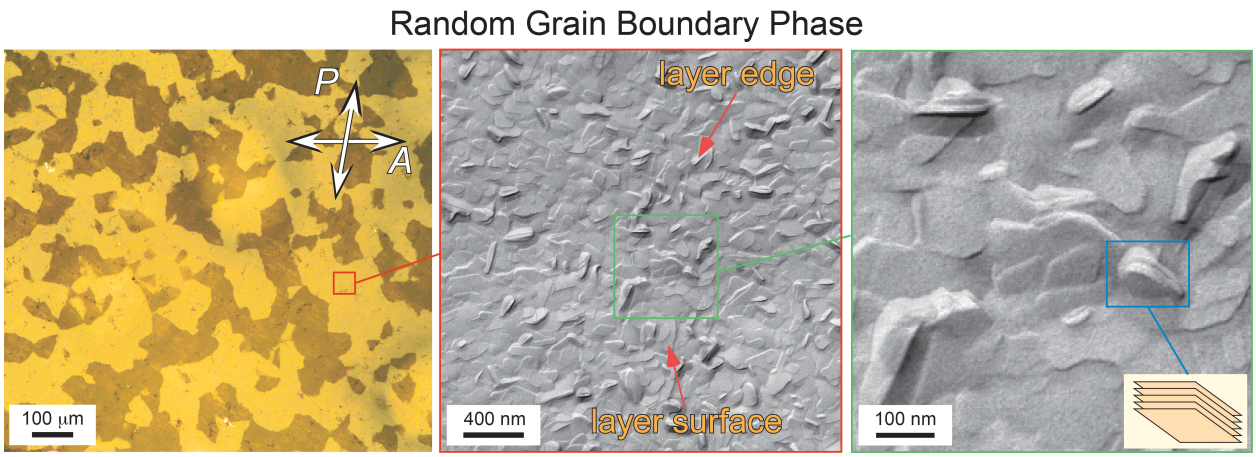

Chiral random grain boundary phase of achiral hockey-stick liquid crystals showing randomly oriented smectic blocks with flat smectic layers.

Journal Name

RSCPublishing

ARTICLE

Chiral Random Grain Boundary Phase of Achiral Hockey-stick Liquid Crystals

Cite this: DOI: 10.1039/x0xx00000x

Dong Chen[a+], Haitao Wang[b+], Min Li[b*], Matthew A. Glaser[a], Joseph E. Maclennan[a], and Noel A. Clark[a**]

Received 00th January 2012,
Accepted 00th January 2012

DOI: 10.1039/x0xx00000x

www.rsc.org/

A disordered chiral conglomerate, the random grain boundary (RGB) phase, has been observed below the smectic A liquid crystal phase of an achiral, hockey-stick molecule. In cells, the RGB phase appears dark between crossed polarizers but decrossing the polarizers reveals large left- and right-handed chiral domains with opposite optical rotation. Freeze-fracture transmission electron microscopy reveals that the RGB phase is an assembly of randomly oriented blocks of smectic layers, an arrangement that distinguishes the RGB from the dark, chiral conglomerate phases of bent-core mesogens. X-ray diffraction indicates that there is significant layer shrinkage at the SmA–RGB phase transition, which is marked by the collapse of layers with long-range order into small, randomly oriented smectic blocks.

Introduction

Molecular structure plays an important role in the self-assembly of liquid crystal phases.[1] Due to their anisotropic molecular shape, rod-like molecules form fluid liquid crystal phases such as the nematic, smectic A, and smectic C.[2] When the molecules are chiral, the mirror symmetry of the liquid crystal phases is removed and molecular self-assemblies with characteristic properties associated with the chirality emerge. For example, the molecular chirality is expressed through the twisting of the director field in the blue, cholesteric, and twist grain boundary phases and through the formation of a director helix in the smectic C. Chirality also leads to ferroelectricity in the smectic C* phase of chiral, rod-like molecules.[3,4] In recent years, the self-organization of bent-core molecules into novel phases different from those exhibited by rod-like molecules has drawn intense attention,[5,6,7,8] stimulated early on by the discovery of spontaneous symmetry breaking in fluid smectics of achiral, bent-core mesogens.[9] Many novel phases unique to bent molecules, such as the B1–B8,[5,6] helical nanofilament,[10] dark conglomerate,[11] polar smectic A,[12] biaxial nematic,[13,14] and twist-bend nematic phases[15,16,17,18,19] have been discovered and characterized. When bent-core mesogens self-assemble into layers, the interplay of molecular tilt and polarization causes the layers to be chiral.[20] The helical nanofilament and dark conglomerate phases of achiral, bent-core molecules are chiral phases that exhibit large homochiral domains that are dark under crossed polarizers but transmit light when the polarizers are decrossed because of optical rotation.[10,11]

Hockey-stick molecules, which are structurally intermediate between rod-like mesogens and true bent-core liquid crystals, also show unusual phases and are of contemporary interest for the design of new materials with useful applications and also for the insights they offer into the fundamental understanding of the self-organization of soft-matter.[21,22,23,24,25,26,27,28,29,30] These molecules typically comprise a central core to which arms of substantially different length are attached. Hockey-stick mesogens exhibit several exotic phases and effects associated with their asymmetric shape, including the dual-characteristic nematic phase (which displays both calamitic and bent-core properties),[31] the occurrence of two polymorphic, tilted smectic phases (the SmC_S and SmC_A phases) induced by a molecular conformation change,[32,33,34] the coexistence of two different molecular tilts at the nematic–SmC transition,[35] the macroscopically chiral nematic and dark conglomerate phases,[36] the frustrated blue and twist grain boundary phase induced by chiral, rod-like mesogens,[37] and a layer thinning transition.[38]

In this paper, we report a new hockey-stick mesogen (COBOXD), an achiral molecule with a flexible alkyl chain attached to one end of an asymmetric, rigid, bent core. A chiral, dark conglomerate phase of randomly oriented smectic blocks, which we call the random grain boundary (RGB) phase, represents a new addition to the rich palette

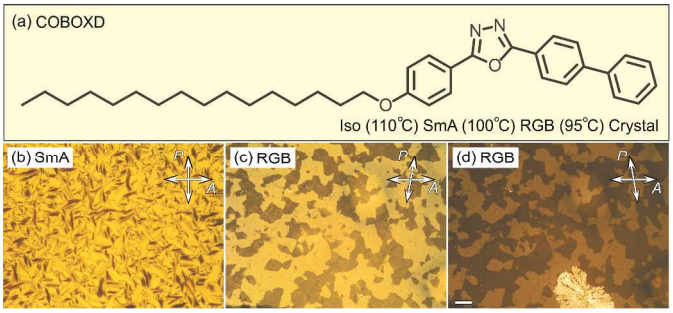

Figure 1: Molecular structure, phase sequence and optical textures of achiral, hockey-stick mesogen. (a) Chemical structure and phase sequence of COBOXD. (b) Polarized light microscope image of the SmA phase at T=110°C, showing fan-like texture with dark brushes parallel to the polarizers. (c) Optical texture of the RGB phase at T=100°C. This phase appears dark between crossed polarizers but left- and right-handed chiral domains can be distinguished by decrossing the polarizers. (d) The crystal phase (bright region) grows in at lower temperature. The scale bar in (d) is 100 μm. The contrast in (c) was enhanced in software. The samples are sandwiched between two planchettes of bare glass spaced about 4 μm apart.

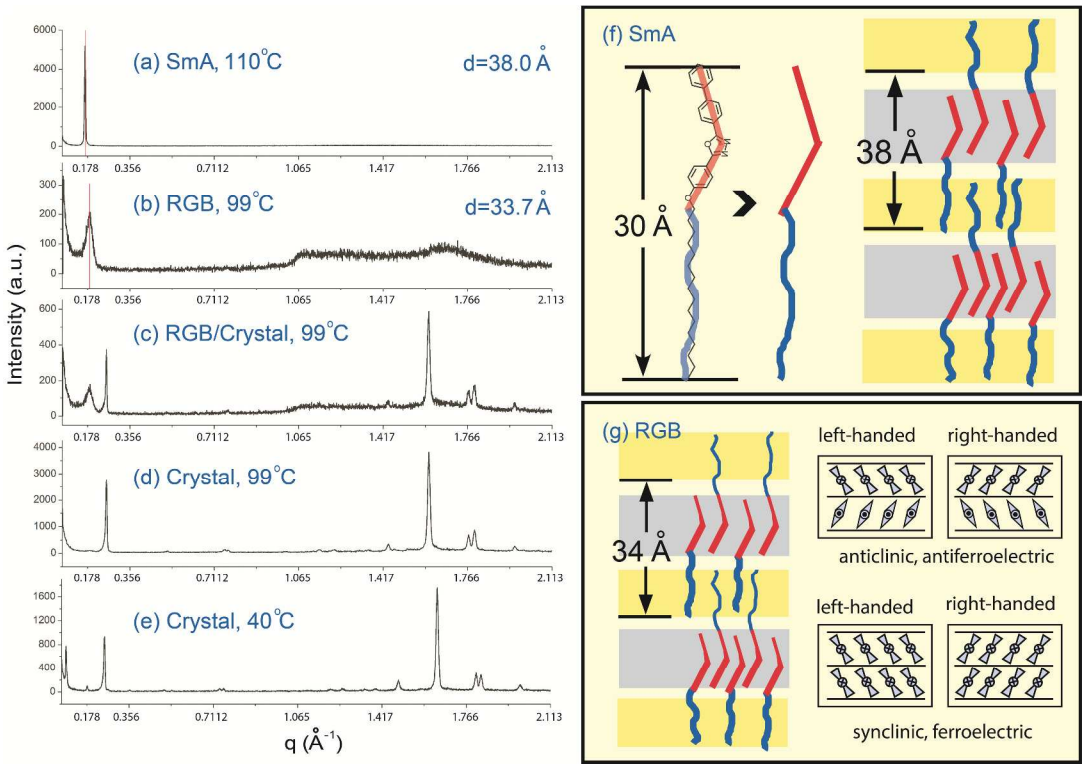

Figure 2: X-ray scattering from COBOXD in (a) the SmA phase, (b) the random grain boundary phase, and (c)-(e) the crystal phase. The layer peak in the SmA phase is sharp, indicating long-range correlations, whereas the scattering in the RGB phase is diffuse, indicating short-range layer correlations. The crystal phase shows multiple sharp peaks at both small and wide angles. (f) The layer spacing of the SmA phase (d~38 Å) is larger than the computed molecular length (l~30 Å) and an interdigitated, bilayer structure is proposed for this phase. (g) The layer spacing in the RGB phase (d~33.7 Å) is smaller than in the SmA phase (d~38 Å), suggesting a tilted phase. The tilt is indicated by the thin (away from the reader) and thick (close to the reader) lines. The molecular arrangement in the smectic layer must be either anticlinic and antiferroelectric or synclinic and ferroelectric to produce the layer chirality. The symmetry of the smectic layers made of interdigitated, tilted hockey-stick molecules is essentially the same as that of bent-core molecules.

of self-assembled microstructures exhibited by liquid crystal molecules.

Experimental Results and Discussion

COBOXD was synthesized using intramolecular dehydration cyclization of the dihydrazide derivative, *N*-(4-cetyloxybenzoyl)-*N*'-(4'-biphenyl carbonyl) hydrazine (C16-Ph).[39] Details of the synthesis are given in Schematic S.1 (Supporting Information). The chemical structure and phase sequence of COBOXD are shown in Figure 1a. Upon cooling, the SmA phase appears from the isotropic, forming fan-like focal-conic textures with the optic axis normal to the layers (Figure 1b). On further cooling, the SmA phase transitions to the RGB phase, the birefringence disappears, and the cell becomes dark under crossed polarizers. Macroscopic left- and right-handed chiral domains may be distinguished by decrossing the polarizers, as shown in Figures 1c and d. Below the RGB phase, the sample becomes crystalline (Figure 1d and Figure S.1a, Supporting Information). The texture of the hockey-stick RGB phase resembles that of the dark, chiral phase of true bent-core mesogens but the mesomorphism is different,[36] since with achiral, bent-core molecules the dark conglomerate phase usually appears directly from the isotropic and the helical nanofilament phase is typically the lowest temperature liquid crystal phase.

The x-ray scattering on cooling is shown in Figures 2a-e. The Bragg reflection from the smectic layers (q~0.164 Å^{-1}, corresponding to a layer spacing d~38.0 Å) in the SmA phase is sharp (Figure 2a), indicating long-range ordering of the layers. The observed SmA layer spacing is substantially larger than the molecular length of COBOXD, l~30.2 Å obtained from Chem3D (MM2, energy minimization), suggesting partial overlapping of the hockey-stick mesogens in this phase (Figure 2f), similar to interdigitated bilayer structures reported previously.[12,40] At lower temperature, in the RGB phase, the x-ray scattering (Figure 2b) shifts to higher wavevector (q~0.186 Å^{-1}, d~33.7 Å). The layer spacing in the RGB phase is thus smaller than that of the SmA phase. The reduced layer spacing could arise partly from an increase in the degree of intercalation in the RGB phase. However, since the phase is chiral, the molecules in the layers must be tilted in order to produce the layer chirality (Figure 2g). If we ignore possible changes of the degree of intercalation, the reduced layer spacing indicates a large molecular tilt in the RGB phase of □□□ cos^{-1}(d/l)~27.5°. In addition, the x-ray scattering of the RGB phase is much more diffuse than that of the SmA phase, which indicates that the correlation length of the smectic layers in the RGB phase is finite and is much shorter than that in the SmA phase. In the crystal phase, sharp x-ray reflection peaks are observed at both small and large angles (Figures 2c-e), suggesting a three-dimensional, ordered structure, consistent with the features observed in free-surface transmission electron microscopy (TEM) images (Figure S.1b, Supporting Information).

The structures observed at the free surface of droplets of liquid crystal in air are typically more ordered than in the bulk because of the lower symmetry imposed by the interface.[41] In the RGB phase, however, TEM images at the air/liquid crystal interface reveal a

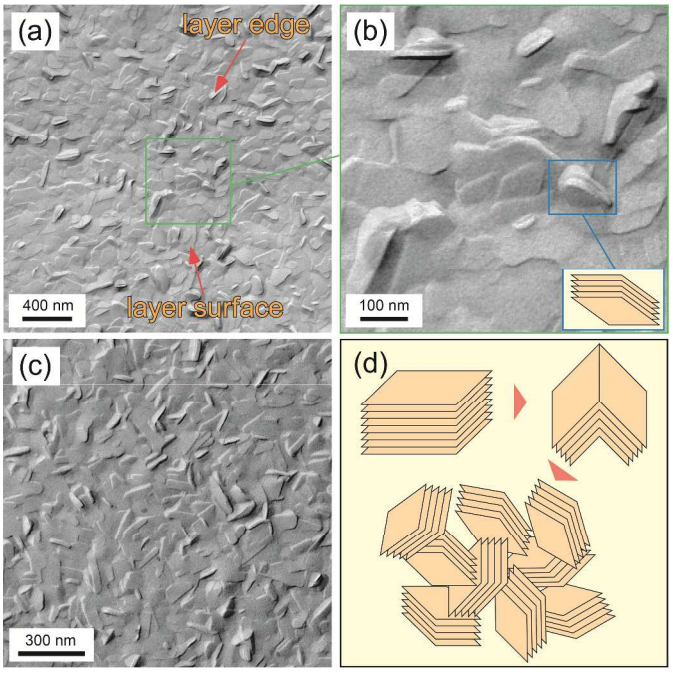

Figure 3: Free-surface and bulk freeze-fracture TEM images of the chiral, dark conglomerate RGB phase. (a) At the air/liquid crystal interface, the RGB phase appears rough, with blocks of smectic layers oriented in different directions. (b) Higher magnification of (a) with a tilted smectic block sketched in the inset. (c) FFTEM image of the RGB phase fractured in the bulk, showing randomly oriented blocks of smectic layers, consistent with the microstructure observed at the free surface. (d) Cartoon showing the evolution of flat, long-range-ordered smectic layers in the SmA phase to disordered blocks in the RGB phase. At the SmA–RGB transition, the layers shrink substantially and break into randomly-oriented blocks. The samples were quenched at T=100°C.

rough surface made of randomly oriented smectic blocks with flat smectic layers (Figures 3a and b) that is very similar to the bulk microstructure observed using freeze-fracture TEM (Figure 3c).[42] The finite size of the smectic blocks observed using TEM is consistent with the diffuse x-ray diffraction of the RGB phase. The orientational disorder of the blocks averages out the birefringence, causing the phase to be optically isotropic.

The microstructure of the RGB phase is fundamentally different from the two known dark, chiral phases formed by achiral, bent-core liquid crystals: the dark conglomerate (DC) phase, made of disordered focal conics, and the helical nanofilament (HNF) or B4 phase, composed of twisted smectic layer ribbons. The structure of both of these phases is dominated by saddle-splay curvature of the layers driven by the intra-layer structural mismatch of the top and bottom molecular arms.[10, 11] Though the symmetry of the smectic layers made of tilted hockey-stick molecules is essentially the same as that of bent-core molecules (Figure 2g), the molecules are interdigitated in each smectic layer in the RGB phase and there is no intra-layer structural mismatch to drive the saddle-splay deformation. The layers within each block are essentially flat in the RGB phase.

The formation of the globally disordered smectic blocks may be understood by considering the difference in molecular packing in the SmA and RGB phases. The SmA–RGB phase transition is marked by the development of large molecular tilt and significant layer shrinkage, as indicated by the x-ray scattering. We propose that this causes the long-range ordered smectic A layers to collapse into small, randomly oriented smectic blocks (Figure 3d). The size of each smectic block is about 200 nm, estimated from the FFTEM images. However, the existence of large chiral domains in the RGB phase implies that chiral symmetry breaking associated with correlated tilting of the director at the phase transition occurs over an extended area before the sample breaks up into blocks.

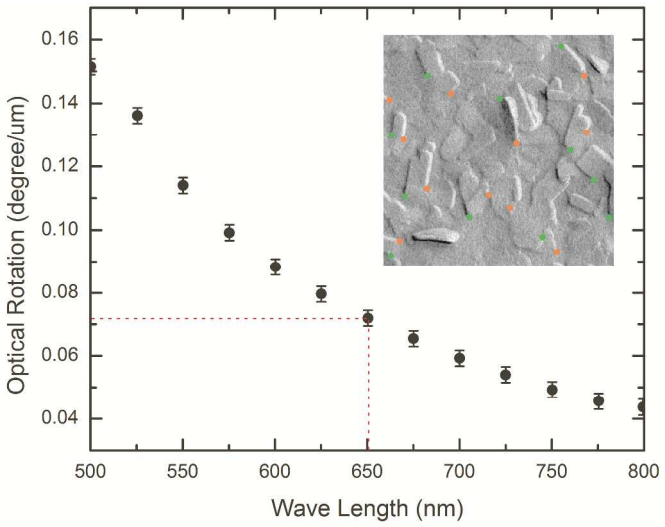

Figure 4: Optical rotation of the RGB phase measured at T=100°C in a 4 μm cell. The optical rotation results purely from the layer chirality, there being no macroscopic twisted structure in this phase. The left- (orange dots) and right-handed (green dots) screw dislocations appear as pairs (inset). The measured optical rotation (OR~0.07 °/μm at λ~650 nm) is consistent with the theoretical prediction of bent-core mesogens (OR_{max}=0.05°/μm, for the SmC_SP_F phase and OR_{max}=0.1°/μm, for the SmC_AP_A phase),[44] a value much smaller than observed in the helical nanofilament phase (OR~0.5 °/μm at λ~650nm[10]).

The smectic layer blocks observed in the RGB phase are reminiscent of those seen in the twist grain boundary (TGB) phase of chiral, rod-like molecules. In the TGB phase, the competition between chiral twisting of the director and the tendency for uniform smectic layering is accommodated by the creation of blocks of smectic layers separated by arrays of screw dislocations that form a helical superstructure with the twist axis parallel to the layers.[43] While the hockey-stick molecules themselves are achiral, the RGB phase has layer chirality, resulting from the interplay of molecular shape, tilt and polarization familiar from conventional bent-core molecules.[20] The chiral twisting power arising from the layer chirality is apparently much smaller than that resulting from the molecular chirality in the TGB phase and no helical superstructure is observed in the RGB phase.

The optical rotation of the RGB phase, measured by finding the extinction orientation of polarized, transmitted light by decrossing the analyzer, is shown in Figure 4. As with many other chiral molecules and phases, the optical rotation increases at shorter wavelengths. The origin of the optical activity could be attributed to either a helical superstructure or the layer chirality produced by simultaneous tilt and polar ordering of the molecules in the smectic layers. We have not, however, observed any macroscopic chiral structures and the left- and right-handed screw dislocations appear as pairs (Figure 4, inset). The measured optical rotation (OR~0.07°/μm at λ=650 nm) is comparable to the experimental and predicted values of chiral smectic layers of tilted, achiral, bent-core molecules (OR_{max}=0.05°/μm, for the SmC_SP_F phase and OR_{max}=0.1°/μm, for

the SmC_AP_A phase[44]) but is much smaller than in the helical nanofilament phase (OR=0.5°/μm at λ=650 nm), where the helical superstructure contributes substantially to the optical activity. We conclude that the optical rotation of the RGB phase results only from the layer chirality and there is no contribution from global chiral structures.

Dark, chiral conglomerate phases have been reported in other achiral, hockey-stick molecules.[36,45,46] These phases typically occur below a nematic or smectic A phase, exhibit large homochiral domains that show optical rotation, and crystallize at lower temperature. It is not known whether any of these phases might also have the RGB structure. Some reported features indicate that they are similar. For example, in the experiments reported by Zafiropoulos et al.,[46] the SmA phase (d=37.7 Å, corresponding to the molecular length in its most extended conformation) is well aligned under a magnetic field of 4 T but the 2D X-ray scattering becomes disordered when it transforms on cooling into the dark, chiral conglomerate SmX phase (d=33.7 Å, indicating a titled phase). The hockey-stick literature shows that in additional to the sponge and helical nanofilament phases of bent-core liquid crystals, the dark, chiral conglomerates phases adopt several other self-assembled microstructures, depending on the shape of the molecules. An example is the chiral, conglomerate phase observed in liquid crystal materials with azobenzene units,[47,48,49] where it has been shown that the azo groups favour the formation of a dark conglomerate phase in which the chains of the azobenzene containing bent-core mesogens are disordered, allowing a denser and more ordered packing of the aromatic cores that leads to a reduced molecular twist and a stronger layer deformation.

Conclusions

The mesophases of an achiral, hockey-stick molecule have been studied. In the SmA phase, the molecules form an interdigitated bilayer structure. On cooling, the SmA phase transitions to a chiral, dark conglomerate we call the random grain boundary phase. Unlike the chiral, dark conglomerate phases of achiral, bent-core molecules, which are dominated by saddle-splay curvature and driven by intra-layer structural mismatch, the RGB phase is an assembly of blocks of flat smectic layers with random orientations. Large chiral domains with weak optical rotation are observed in cells but freeze-fracture TEM reveals no macroscopic chiral structure. The RGB phase thus shows optical behavior similar to that of achiral, bent-core mesogens but has a microstructure more similar to that of chiral, rod-like molecules, making it different from any previously known phases. These properties are presumably a manifestation of the hockey-stick shape of the mesogens, which are an interesting class of molecules straddling the border between rod-like and bent-core liquid crystals.

Acknowledgements

This work was supported by NSF MRSEC Grant DMR-0820579. Use of the National Synchrotron Light Source was supported by the U.S. Department of Energy, Divisions of Materials and Chemical Sciences. This work was also supported by National Science Foundation of China (51103057, 51073071).

Notes and references

[a] Department of Physics and Liquid Crystal Materials Research Center, University of Colorado, Boulder, CO 80309-0390.
[b] Address here. Key Laboratory of Automobile Materials (MOE) & College of Materials Science and Engineering, Jilin University, Changchun 130012, China.
[+]These authors contributed equally to this work
[*]Email: minli@jlu.edu.cn
[**]Email: noel.clark@colorado.edu

Electronic Supplementary Information (ESI) available: [details of the material synthesis and additional optical and FFTEM images]. See DOI: 10.1039/b000000x/

1 C. Tschierske, *Angew. Chem. Int. Ed.*, 2013, **52**, 8828.
2 P. G. de Gennes and J. Prost, The Physics of Liquid Crystals, Oxford Univ. Press, New York, 2nd edition, 1993.
3 R. B. Meyer, L. Liebert, L. Strzelecki and P. Keller, *Journal de Physique Letters*, 1975, **36**, L69.
4 N. A. Clark and S. T. Lagerwall, *Appl. Phys. Lett.*, 1980, **36**, 899.
5 H. Takezoe and Y. Takanishi, *Jpn. J. Appl. Phys.*, 2006, **45**, 597.
6 R. A. Reddy and C. Tschierske, *J. Mater. Chem.*, 2006, **16**, 907.
7 J. Etxebarria and M. B. Ros, *J. Mater. Chem.*, 2008, **18**, 2919.
8 A. Eremin and A. Jákli, *Soft Matter*, 2013, **9**, 615.
9 T. Niori, T. Sekine, J. Watanabe, T. Furukawa and H. Takezoe, *J. Mater. Chem.*, 1996, **6**, 1231.
10 L. E. Hough, H. T. Jung, D. Krüerke, M. S. Heberling, M. Nakata, C. D. Jones, D. Chen, D. R. Link, J. Zasadzinski, G. Heppke, J. P. Rabe, W. Stocker, E. Körblova, D. M. Walba, M. A. Glaser and N. A. Clark, *Science*, 2009, **325**, 456.
11 L. E. Hough, M. Spannuth, M. Nakata, D. A. Coleman, C. D. Jones, G. Dantlgraber, C. Tschierske, J. Watanabe, E. Körblova, D. M. Walba, J. E. Maclennan, M. A. Glaser and N. A. Clark, *Science*, 2009, **325**, 452.
12 R. A. Reddy, C. Zhu, R. Shao, E. Korblova, T. Gong, Y. Shen, E. Garcia, M. A. Glaser, J. E. Maclennan, D. M. Walba and N. A. Clark, *Science*, 2011, **332**, 72.
13 S.Chakraborty, J. T. Gleeson, A. Jákli and S. Sprunt, *Soft Matter*, 2013**, 9,** 1817.
14 C. Tschierske and D. J. Photinos, *J. Mater. Chem.*, 2010**, 20**, 4263.
15 I. Dozov, *Europhys. Lett.*, 2001, **56**, 247.
16 C. T. Imrie and P. A. Henderson, *Chem. Soc. Rev.*, 2007, **36**, 2096.
17 K. Adlem, M. Čopič, G. R. Luckhurst, A. Mertelj, O. Parri, R. M. Richardson, B. D. Snow, B. A. Timimi, R. P. Tuffin and D. Wilkes, *Phys. Rev. E*, 2013, **88**, 022503.
18 D. Chen, J. H. Porada, J. B. Hooper, A. Klittnick, Y. Shen, M. R. Tuchband, E. Korblova, D. Bedrov, D. M. Walba, M. A. Glaser, J. E. Maclennan and N. A. Clark, *Proc. Natl. Acad. Sci.*, 2013, **110**, 15931.
19 V. Borshch, Y.-K. Kim, J. Xiang, M. Gao, A. Jákli, V. P. Panov, J. K. Vij, C. T. Imrie, M. G. Tamba, G. H. Mehl and O. D. Lavrentovich, *Nature Communications*, 2013, **4**, 2635.
20 D. R. Link, G. Natale, R. Shao, J. E. Maclennan, N. A. Clark, E. Körblova and D. M. Walba, *Science*, 1997, **278**, 1924.
21 R. Cristiano, A. Alexandre Vieira, F. Ely and H. Gallardo, *Liquid Crystals*, 2006, **33**, 381.
22 F. C. Yu and L. J. Yu, *Liquid Crystals*, 2008, **35**, 799.
23 W. Weissflog, U. Dunemann, S. Findeisen-Tandel, M. Gabriela Tamba, H. Kresse, G. Pelzl, S. Diele, U. Baumeister, A. Eremin, S. Stern and R. Stannarius, *Soft Matter*, 2009, **5**, 1840.

24 E. Enz, S. Findeisen-Tandel, R. Dabrowski, F. Giesselmann, W. Weissflog, U. Baumeister and J. Lagerwall, *J. Mater. Chem.*, 2009, **19**, 2950.
25 S. Radhika, H.T. Srinivasa and B.K. Sadashiva, *Liquid Crystals*, 2011, **38**, 785.
26 E.-R. Cioanca, E. L. Epure, I. Carlescu, G. Lisa, D. Wilson, N. Hurduc, and D. Scutaru, *Mol. Cryst. Liq. Cryst.*, 2011, **537**, 51.
27 P. Sathyanarayana, S. Radhika, B. K. Sadashiva and S. Dhara, *Soft Matter*, 2012, **8**, 2322.
28 M. Horčic, V. Kozmík, J. Svoboda, V. Novotná and D. Pociecha, *J. Mater. Chem. C*, 2013, **1**, 7560.
29 D. Wu, F. Feng, D. Xie, Y. Chen, W. Tan and K. S. Schanze, *J. Phys. Chem. Lett.* 2012, **3**, 1711.
30 D. Wu and K. S. Schanze, ACS Appl. Mater. Interfaces 2014, **6**, 7643.
31 A. Chakraborty, M. Kumar Das, B. Das, U. Baumeister and W. Weissflog, *J. Mater. Chem. C*, 2013, **1**, 7418.
32 B. Das, S. Grande, W. Weissflog, A. Eremin, M. W. Schröder, G. Pelzl, S. Diele and H. Kresse, *Liq. Cryst.*, 2003, **30**, 529.
33 V. Novotná, J. Žurek, V. Kozmík, J. Svoboda, M. Glogarová, J. Kroupa and D. Pociecha, *Liq. Cryst.*, 2008, **35**, 1023.
34 A. Chakraborty, B. Das, M. K. Das, S. Findeisen-Tandel, M.-G. Tamba, U. Baumeister, H. Kresse and W. Weissflog, *Liq. Cryst.*, 2011, **38**, 1085.
35 L. Chakraborty, N. Chakraborty, D. Debnath Sarkar, N. V. S. Rao, S. Aya, K. Van Le, F. Araoka, K. Ishikawa, D. Pociecha, E. Gorecka and H. Takezoe, *J. Mater. Chem. C*, 2013, **1**, 1562.
36 A. Belaissaoui , S. J. Cowling and J. W. Goodby, *Liquid Crystals*, 2013, **40**, 822.
37 V. Novotná, M. Glogarová, V. Kozmík, J. Svoboda, V. Hamplová, M. Kašpara and D. Pociecha, *Soft Matter*, 2013, **9**, 647.
38 M. Kr. Paul, R. K. Nath, B. Moths, L. Pan, S. Wang, R. Deb, Y. Shen, N. V. S. Rao and C. C. Huang, *Phase Transitions*, 2012, **85**, 1070.
39 D. M. Pang, H. T. Wang and M. Li, *Tetrahedron*, 2005, **61**, 6108.
40 T. J. Dingemans, N. Sanjeeva Murthy and E. T. Samulski, *J. Phys. Chem. B*, 2001, **105**, 8845.
41 D. Chen, R. Shao, J. E. Maclennan, M. A. Glaser, E. Korblova, D. M. Walba, N. Gimeno, M. Blanca Ros and N. A. Clark, *Liquid Crystals*, 2013, **40**, 1730.
42 D. Chen, D. K. Yoon, J. E. Maclennan, M. A. Glaser, E. Korblova, D. M. Walba, N. Gimeno, M. B. Ros, R. Deb, N. V. S. Rao and N. A. Clark, *Soft Matter*, 2013, **9**, 11303.
43 J. Fernsler, L. Hough, R.-F. Shao, J. E. Maclennan, L. Navailles, M. Brunet, N. V. Madhusudana, O. Mondain-Monval, C. Boyer, J. Zasadzinski, J. A. Rego, D. M. Walba and N. A. Clark, *PNAS*, 2005, **102**, 14191.
44 L. E. Hough, C. Zhu, M. Nakata, N. Chattham, G. Dantlgraber, C. Tschierske and N. A. Clark, *Phys. Rev. Lett.*, 2007, **98**, 037802.
45 T. J. Dingemans and E. T. Samulski, *Liquid Crystals*, 2000, **27**, 131.
46 N. A. Zafiropoulos, W. Lin, E. T. Samulski, T. J. Dingemans and S. J. Picken, *Liquid Crystals*, 2009, **36**, 649.
47 M. Alaasar, M. Prehm and C. Tschierske, *Chem. Commun.*, 2013, **49**, 11062.
48 M. Alaasar, M. Prehm, M. Brautzsch and C. Tschierske, *J. Mater. Chem. C*, 2014, **2**, 5487.
49 A. Zep, K. Sitkowska, D. Pociecha and E. Gorecka, *J. Mater. Chem. C*, 2014, **2**, 2323.